Transverse modes of a diode-laser pumped monolithic unidirectional non-planar ring laser

Keying Wu (吴克瑛)[1], Suhui Yang (杨苏辉)[2], and Guanghui Wei (魏光辉)[2]

[1]*Department of Electronic Engineering, Tsinghua University, Beijing 100084*

[2]*Department of Optical Engineering, Beijing Institute of Technology, Beijing 100081*

Received August 8, 2002

Diode-laser pumped monolithic single-frequency non-planar ring laser has the advantages of compactness, reliability and high efficiency. But when the pump power is high enough, the thermal effect will be serious and the high-order transverse modes will appear. Therefore the single-mode output power is limited. In this paper, the mechanism of generating the high-order transverse modes in the monolithic unidirectional non-planar ring cavity is analyzed using ray tracing method. The calculated results are in agreement with the experiments.

OCIS codes: 140.6810, 140.3410, 140.3480.

Kane and Byer reported monolithic non-planar Nd:YAG ring laser in 1985[1] and achieved the single-frequency oscillation by a diode-pumped ring laser with dimensions of $12 \times 9 \times 3$ mm^3 in 1987[2]. Freitag, Tünnermann *etal.* have investigated this kind of lasers[3–7] and 2 W single-frequency output power has been obtained[3]. We have achieved more than 600-mW stable single-frequency continuous wave from the monolithic non-planar ring lasers fabricated by our own special technology[10]. Despite there are many advantages of the diode-pumped monolithic non-planar ring laser, its highest single-frequency output power is limited by the thermal lens effect. When the pump power is high enough, the thermal effect of the laser resonator will be serious and the high-order transverse modes will appear. So far as we known, no paper has analyzed the high-order transverse mode in this kind of cavity. In this paper, the ray tracing method is used to analyze the influence of the thermal lens effect and the pumping beam misalignment on the mode distribution in the non-planar cavity.

Figure 1 is the monolithic non-planar ring laser cavity in the supposed space coordinate system. The crystal is end-pumped by a diode laser and is placed in a magnetic field **H**. The oscillating wave travels unidirectionally in the cavity. Ideally, the ray starts from A and travels along AB, it is totally internal reflected at the points B, C, D and back to A. The next circle is the same as the first.

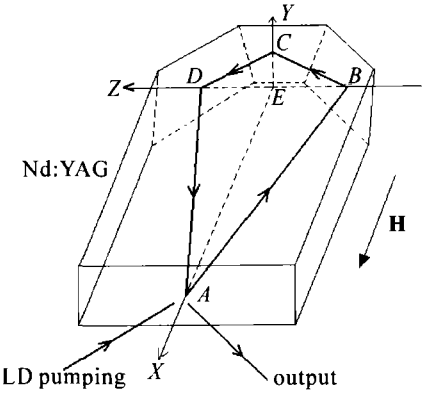

Fig. 1. Monolithic non-planar ring laser.

The plane BCD is perpendicular to the plane ABD. E is the middle point of BD and is chosen to be the coordinate origin.

Practically, the laser energy in the cavity distributes as transverse modes. It could be considered as a group of straight rays. A ray is supposed to start from the point A_1 with a small displacement from the ideal point A. This displacement is denoted by its coordinate values on Y-axes and Z-axes as a_{y1} and a_{z1}. The initial ray deviates from the ideal direction of AB with a small angle of $\Delta\theta$, whose projections in $y = 0$ and $z = 0$ plane is $\Delta\theta_{y1}$ and $\Delta\theta_{z1}$, respectively. After travelling several circles inside the cavity, the light ray comes back to output surface with the incident point A_{i+1}. Subscript i is the tracing circle time. The distribution of the aggregate A_i on the output surface of the crystal gives some information of the transverse mode and its cavity loss. If the aggregate of A_i has more elements in the end-pumping area, the transverse mode constituted by this light ray gets higher gain and oscillates easier.

The relationship of the vectors in reflection scheme of Fig. 2 can be expressed as

$$\mathbf{i} - 2(\mathbf{i} \cdot \mathbf{n})\mathbf{n} = \mathbf{r}, \tag{1}$$

where $\mathbf{i}$ is the unit vector of the incident ray, $\mathbf{r}$ is the unit vector of the reflected ray and $\mathbf{n}$ is the unit vector of the surface normal.

It is supposed that the thermal lens induced by the end-pumping laser is a thin lens with its center at the point of A and its focus on the line of AB. It is also supposed that the thermal lens only affects the direction of the ray of A_iB_i. As Fig. 3 shows, the vector $\mathbf{l}$ has its origin of point A and is parallel to the reflected vector of the point A_i unaffected by thermal lens. After the thermal

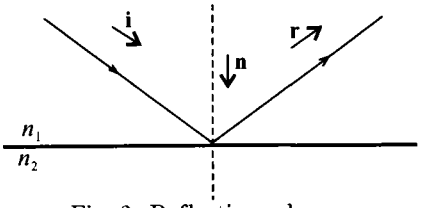

Fig. 2. Reflection scheme.

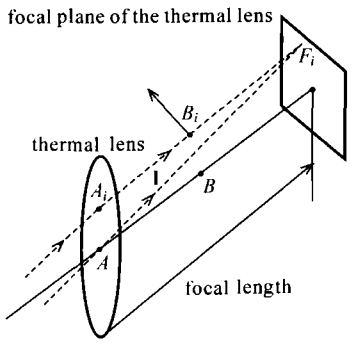

Fig. 3. The thermal lens effect on the direction of A_iB_i.

lens, the ray changes its direction of **l** to A_iF_i. F_i is the intersection point of **l** and the focal plane of the thermal lens. B_i is the intersection point of A_iF_i and the crystal surface.

Figure 4 is the calculated results as the initial light ray departing from the ideal initial point A or deviating from the ideal direction AB, respectively. For each cases, the light ray travels inside the cavity with 500 round trips and strikes the output surface 500 times ($i = 1, 2, 3, \cdots, 500$). Figures 4(a) and (b) display the results with $a_{y1} = 0$, $a_{z1} = 0.1$ mm, $\Delta\theta_y = \Delta\theta_z = 0$ and the focal length of the thermal lens being infinite and 100 mm. With infinite focal length, the reflected points on the output surface distribute like a circle with radius of 0.1 mm. Figure 4(b) shows that with some degree of the thermal lens effect, the points remain in the scope with the radius of 0.1 mm. Therefore, the suitable thermal lens could help the fundamental transverse-mode, which constituted mostly by the rays parallel with AB, resonate stably in the crystal. Figures 4(c) and (d) show the results with $a_{y1} = 0$, $a_{z1} = 0$ mm, $\Delta\theta_y = 0.001$ deg, $\Delta\theta_z = 0$ and the focal length of the thermal lens being infinite and 3000 mm. With the infinite focal length, the reflected points on the output surface radiate from the point of A. There is no limit to the A_i as increasing the number of the round trips. When the thermal focal length is definite but larger than the optical path length of the resonator ring (The ring length of our own cavity is 29.9 mm), the non-planar resonator is stable and the ray with a small $\Delta\theta$ could resonate in the cavity. More calculations with different focal lengths denote that, in the stable cavity, the area radius of the aggregate of A_i (the number of the elements is 500) decreases with the shorter focal length.

Figure 5 displays some other interesting results under different initial conditions. From a lot of simulating calculations, it is found that the figures of the reflected points on the output surface are prone to be like one or more rings or to have five similar parts.

In our experiments, as the end-pumping beam is collimated perfectly, the strong thermal lens in the case of strong power pumping is the main reason for high-order transverse mode and multi-frequency appearance. Figure 6(c) displays that the fundamental and one of the high-order transverse modes oscillate together. With our own crystal, the single-frequency fundamental transverse-mode will maintain as the output power is up to 600 mW. By adjusting the pumping beam misalignment, the high-order transverse modes can be obtained in the case of lower power pumping as shown in Figs. 6(a), (b) and (d). In most cases, the high-order transverse structures are ring like form or flower like form with five petals. It coincides with the simulated results of Figs. 4 and 5. Adjusting the pumping beam misaligned can obtain the single transverse mode of novel flower petal form. The measrued M^2 factor of this mode is about 2.3.

By using the ray tracing method, the mechanism of the high order transverse modes is described. From the calculated and the experimental results, the following conclusion can be made.

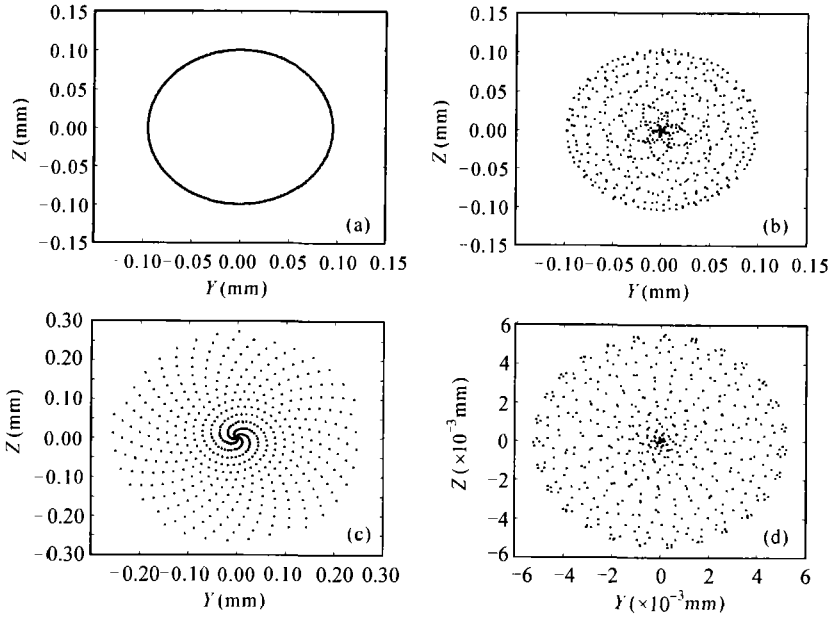

Fig. 4. The pattern of A_i ($i = 1, 2, \cdots, 500$) under the initial condition. f is the thermal focal length. (a) $a_{y1} = 0$, $a_{z1} = 0.1$ mm, $\Delta\theta_y = \Delta\theta_z = 0$, $f = \infty$; (b) $a_{y1} = 0$, $a_{z1} = 0.1$ mm, $\Delta\theta_y = \Delta\theta_z = 0$, $f = 100$ mm; (c) $a_{y1} = 0$, $a_{z1} = 0$ mm, $\Delta\theta_y = 0.001$ deg, $\Delta\theta_z = 0$, $f = \infty$; (d) $a_{y1} = 0$, $a_{z1} = 0$ mm, $\Delta\theta_y = 0.001$ deg, $\Delta\theta_z = 0$, $f = 3000$ mm.

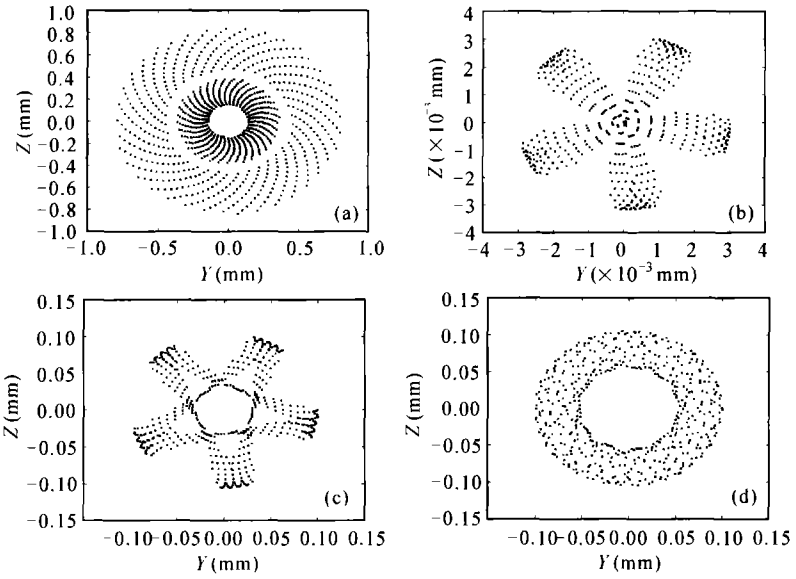

Fig. 5. The results of tracing rays under the different initial conditions ($i = 1, 2, \cdots, 500$). f is the thermal focal length. (a) $a_{y1} = 0.1$ mm, $a_{z1} = 0.1$ mm, $\Delta\theta_y = 0.001$ deg, $\Delta\theta_z = 0$, $f = \infty$. (b) $a_{y1} = 0$, $a_{z1} = 0.1$ mm, $\Delta\theta_y = 0.001$ deg, $\Delta\theta_z = 0$, $f = 1000$ mm. (c) $a_{y1} = 0.1$ mm, $a_{z1} = 0$, $\Delta\theta_y = 0.01$ deg, $\Delta\theta_z = 0$, $f = 1000$ mm. (d)$a_{y1} = 0.1$ mm, $a_{z1} = 0.1$ mm, $\Delta\theta_y = 0.01$ deg, $\Delta\theta_z = 0$, $f = 3000$ mm.

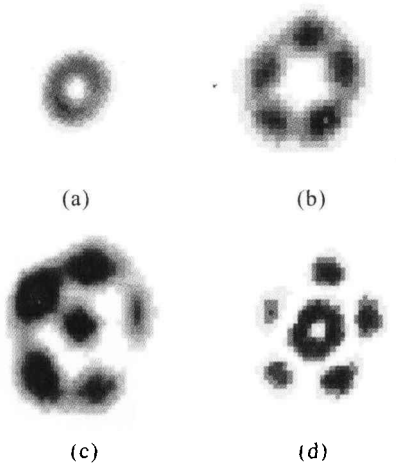

Fig. 6. Transverse modes detected by CCD.

1) The thermal lens plays important role for the laser energy distribution in the monolithic non-planar ring cavity. A reasonable thermal lens makes the cavity stable.

2) The pumping beam misalignment and the thermal lens effect are the reasons of high-order transverse mode appearance. In the monolithic non-planar ring cavity, the distributions of the high-order transverse modes are prone to be ring or to have five similar parts.

We would like to gratefully acknowledge senior engineers Anhan Liu, Zhen Zhu and Tengyu Jiang, engineer Lianrong Cui and Dongmei Hong of North China Research Institute for coating the films, providing and processing the laser crystals, professor Wei Li, Wei Pan of China Iron and Steel Research Institute for supplying the permanent magnet, and Doctor Wei Sun of Beijing Institute of Technology for detection the M^2 factor. K. Wu's e-mail address is wukeying@ee.tsinghua.edu.cn.

References

1. T. J. Kane and R. L. Byer, Opt. Lett. **10,** 65 (1985).
2. T. J. Kane, A. C. Nillsson, and R. L. Byer, Opt. Lett. **12,** 175 (1987).
3. I. Freitag, A. Tünnermann, and H. Welling, Opt. Commun. **15,** 511 (1995).
4. I. Freitag, A. Tünnermann, and H. Welling, Electron. Lett. **33,** 777 (1997).
5. K. Schneider, S. Schiller, J. Mlynek, M. Bode, and I. Frietag, Opt. Lett. **21,** 1999 (1996).
6. M. Bode, I. Freitag, A. Tünnermann, and H. Welling, Opt. Lett. **22,** 1220 (1997).
7. I. Freitag, I. Lörpke, A. Tünnermann, and H. Welling, Opt. Commun. **101,** 371 (1993).
8. K. Y. Wu, C. M. Zhao, J. F. Shi, G. H. Wei, A. H. Liu, L. R. Cui, Z. Zhu, and D. M. Hong, J. Beijing Institute of Technology **10,** 175 (2001).
9. K. Y. Wu, C. M. Zhao, G. H. Wei, and J. F. Shi, Acta Optica Sinica (in Chinese) **20,** 1245 (2000).
10. S. H. Yang, K. Y. Wu, C. M. Zhao, and H. W. Guang, Proc. SPIE **4223,** 1 (2000).
11. S. H. Yang, K. Y. Wu, and G. H. Wei, Chin. Phys. Lett. **18,** 906 (2001).
12. K. Y. Wu, S. H. Yang, C. M. Zhao, and G. H. Wei, Chin. Phys. Lett. **17,** 728 (2000).
13. K. Y. Wu, S. H. Yang, C. M. Zhao, and G. H. Wei, Proc. SPIE **3929,** 323 (2000).
14. K. Y. Wu, S. H. Yang, and G. H. Wei, Opt. Commun. **203,** 323 (2002).
15. K. Y. Wu, S. H. Yang, C. M. Zhao, and G. H. Wei, Proc. SPIE **4223,** 8 (2000).